analytical chemistry

Article

pubs.acs.org/ac

Quantitative Online Liquid Chromatography–Surface-Enhanced Raman Scattering (LC-SERS) of Methotrexate and its Major Metabolites

Abdu Subaihi,[†] Drupad K. Trivedi,[†] Katherine A. Hollywood,[†] James Bluett,[‡,§] Yun Xu,[†] Howbeer Muhamadali,[†] David I. Ellis,[†] and Royston Goodacre*[,†]

[†]School of Chemistry, Manchester Institute of Biotechnology, University of Manchester, 131 Princess Street, Manchester, M1 7DN, U.K.

[‡]Arthritis Research UK Centre for Genetics and Genomics, Centre for Musculoskeletal Research, The University of Manchester, Manchester M13 9PT, U.K.

[§]NIHR Manchester Musculoskeletal BRU, Central Manchester Foundation Trust, Manchester Academic Health Sciences Centre, Manchester, M13 9WU, U.K.

Supporting Information

ABSTRACT: The application of Raman spectroscopy as a detection method coupled with liquid chromatography (LC) has recently attracted considerable interest, although this has currently been limited to isocratic elution. The combination of LC with rapidly advancing Raman techniques, such as surface-enhanced Raman scattering (SERS), allows for rapid separation, identification and quantification, leading to quantitative discrimination of closely eluting analytes. This study has demonstrated the utility of SERS in conjunction with reversed-phase liquid chromatography (RP-LC), for the detection and quantification of the therapeutically relevant drug molecule methotrexate (MTX) and its metabolites 7-hydroxy methotrexate (7-OH MTX) and 2,4-diamino-*N*(10)-methylpteroic acid (DAMPA) in pure solutions and mixtures, including spikes into human urine from a healthy individual and patients under medication. While the RP-LC analysis developed employed gradient elution, where the chemical constituents of the mobile phase were modified stepwise during analysis, this did not overtly interfere with the SERS signals. In addition, the practicability and clinical utility of this approach has also been demonstrated using authentic patients' urine samples. Here, the identification of MTX, 7-OH MTX and DAMPA are based on their unique SERS spectra, providing limits of detection of 2.36, 1.84, and 3.26 μM respectively. Although these analytes are amenable to LC and LC-MS detection an additional major benefit of the SERS approach is its applicability toward the detection of analytes that do not show UV absorption or are not ionised for mass spectrometry (MS)-based detection. The results of this study clearly demonstrate the potential application of online LC-SERS analysis for real-time high-throughput detection of drugs and their related metabolites in human biofluids.

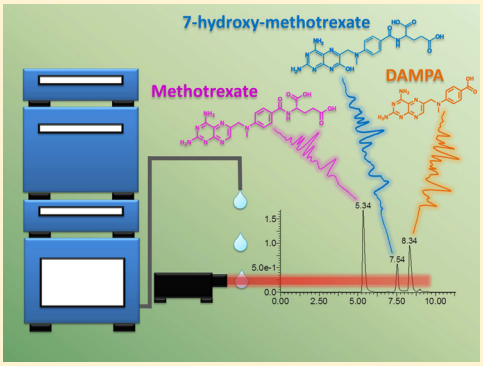

Chemical analysis of complex samples in solution usually involves the separation of a sample followed by identification and quantification of compounds. Common analytical separation techniques involve liquid chromatography (LC), gas chromatography (GC), and capillary zone electrophoresis (CZE).[1] These separation techniques can be readily combined in various chemical detection platforms, including microfluidic devices,[2] spectrometric techniques (UV–vis and fluorescence), and mass spectrometry (MS). MS is commonly accepted as the gold standard detection technique that provides unique identification of analytes based on their mass-to-charge ratio.[3] However, some common challenges often faced in MS detection include the need to ionize the molecule, ion suppression effects, poor discrimination between isobaric compounds, and the requirement for derivatization of some complex samples; these challenges can occasionally limit the use of this approach for characterization.[4−7]

Recently vibrational spectroscopic techniques have become highly attractive as they are nondestructive, inexpensive and can be readily hyphenated with separation techniques including high-performance liquid chromatography (HPLC),[8] and capillary zone electrophoresis (CZE).[9] However, the development of hyphenation between HPLC separation and vibrational spectroscopy-based detection has not progressed significantly over recent years, mainly, as a result of additional complexity introduced by the use of HPLC solvents, which can often mask the analyte signals detected by vibrational spectroscopy. This

Received: March 13, 2017
Accepted: May 15, 2017
Published: May 15, 2017

DOI: 10.1021/acs.analchem.7b00916
Anal. Chem. 2017, 89, 6702–6709

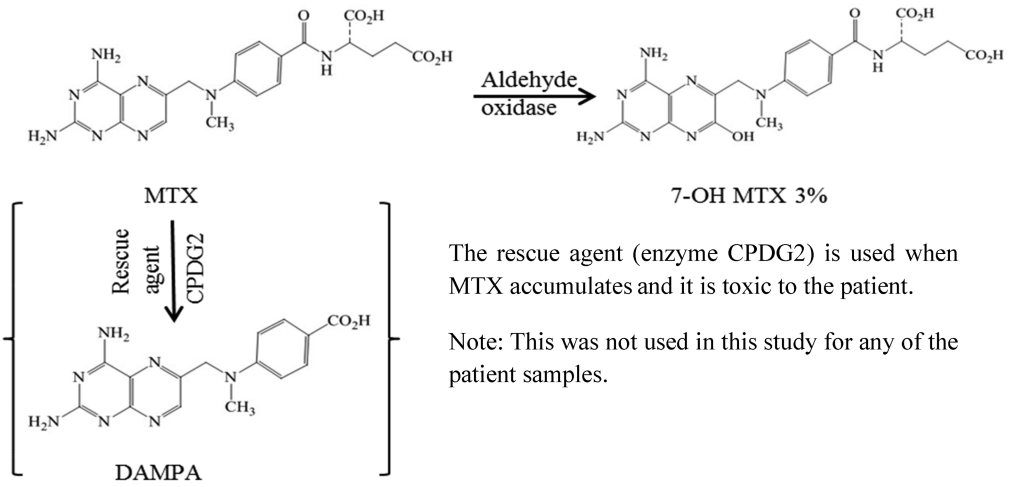

Figure 1. Chemical structures of MTX, 7-OH MTX, and DAMPA.[34,52,53]

can be further compounded when HPLC employs gradient elution where the solvent composition is changed (stepwise or continually) throughout the LC analyses. Although recent advances in data processing approaches allow for the effective removal of solvent backgrounds,[10] which has stimulated this area of research and has the potential to significantly increase the scope of these chromatographic/vibrational hyphenated approaches.

For many applications surface-enhanced Raman scattering (SERS)[11,12] is an attractive approach due to its enhanced sensitivity over other vibrational spectroscopy techniques. SERS provides detailed structural information, allowing for definitive analyte identification with the advantage of rapid analysis. Additionally, the instrumentation is relatively small and inexpensive compared to the other techniques mentioned above.[13,14] Furthermore, SERS enhances the inelastically scattered light because of the presence of a metal surface with nanoscale features, which increase the detection signal by multiple orders of magnitude.[15] The structural information provided by the SERS spectra can also offer a higher molecular specificity alternative for routine analysis of biomolecules. However, SERS can encounter some challenges with multiple analytes in complex biological matrices, such as urine, serum, etc., because of the occurrence of overlapping bands. Using LC coupled with SERS (LC-SERS) can help to overcome these challenges via the efficient separation of the analytes within a complex biological sample prior to SERS detection. Furthermore, LC-SERS can be conducted in real-time (i.e., using online detection), thus allowing for high-throughput sample analysis and data collection that takes no longer than the chromatographic run. In addition, the collection time can be further optimized when data are collected in a targeted fashion with limited predetermined analytes of interest, instead of profiling the entire biofluid. However, there are inherent challenges associated with colloid-based SERS approaches. The nanoparticles need to be introduced into the mobile-phase flow and allowed to mix and aggregate adequately to achieve a maximum SERS response, while at the same time, reducing the distance between the column and detector to prevent sample diffusion and loss of analyte resolution.

Various attempts have been reported previously,[16−20] using different approaches for online and off-line LC-SERS. Cowcher and co-workers demonstrated the application of LC-SERS for the online quantification of purine bases,[8] where the introduction of silver colloid was followed by an aggregation agent into the postcolumn flow of a HPLC system. The study demonstrated limits of detection in the region of 100−500 pmol of purine base concentrations. Such an approach, thus makes online LC-SERS a viable technique for the detection of drugs in biofluids, along with trace metabolites that are routinely only detectable using more sensitive techniques such as mass spectrometry. However, to date, applications of online LC-SERS analyses have been limited and efficient chromatographic separation can improve detection by SERS.[21]

In this work, we have analyzed methotrexate (MTX) and its metabolites in urine using an online reversed-phase LC-SERS setup employing gradient elution. Methotrexate (2,4-diamine-*N*,10-methylpteroyl glutamic acid) is a folate antagonist used for antirheumatic and antineoplastic diseases.[22] Nowadays, with its application for cancer therapy, measurement of MTX is highly recommended in a clinical setting as part of therapeutic drug monitoring (TDM) as MTX can be toxic.[23] MTX is currently administrated in both low- and high-dosage, with high doses (e.g., 1−33 g m^{-2}) used for the treatment of some leukemias and osteosarcomas,[24,25] while much lower doses (e.g., 7.5−20 mg orally once a week) are used for the treatment of conditions, such as psoriasis and rheumatoid arthritis.[26,27] The therapeutic range of MTX for cancer therapy is in the concentration range of micromolar, with the accurate value being strongly based on whether it is administrated as a single agent or in combination with other drugs.[28] The plasma MTX concentration at 48 h after the administration of high doses of MTX infusion should be ≤1 μM, and adverse effects due to toxicity have been associated with concentrations ≥10 μM.[29,30] MTX is poorly metabolized, and most of the dose is excreted unchanged in urine while approximately 3% is converted to 7-hydroxy-methotrexate (7-OH MTX).[31,32] Additionally, as also shown in Figure 1 a single administration of carboxypeptidase (CPDG2) can be used to hydrolyze MTX by degradation into 2,4-diamino-*N*(10)-methylpteroic acid (DAMPA) to allow the patient to remove MTX from their body.[33,34]

Analysis of MTX is routinely performed using the enzyme-multiplied immunoassay technique (EMIT),[35] or by fluorescence polarization immunoassay (FPIA).[36,37] Although these immuno-assays are rapid, they suffer from low specificity, with cross-reaction between MTX metabolites such as DAMPA, and also have a limited range for quantification requiring long sample preparation methods. HPLC methods have been

DOI: 10.1021/acs.analchem.7b00916
Anal. Chem. 2017, 89, 6702−6709

Table 1. Estimated Limits of Detections (LODs) of MTX and 7-OH MTX from Patient Urine Samples Using LC-SERS and LC-UV Detection

		LC-SERS estimate (μM)				LC-UV estimate (μM)			
patient number	dosage (mg)	MTX	SD	7-OH MTX	SD	MTX	SD	7-OH MTX	SD
1	15	8.35	1.39	5.11	1.12	7.75	0.51	6.13	0.91
2	10	8.15	0.92	5.57	1.28	7.34	0.49	5.78	0.63
3	20	5.36	1.18	ND		5.08		ND	
4	20	5.14	0.72	ND		4.96		ND	

[a]Values are the averages of 3 measurements. SD: Standard deviation. ND: Not detected. Note that the MTX dose may not correlate with the LC-SERS or LC-UV estimates of MTX due to personal differences in human metabolism and/or clearance of the drug from the body.

developed for MTX analysis which use fluorometric detection,[38] but this method is subject to interference by folates, rendering it vulnerable to misinterpretation as well as a reduction in sensitivity. HPLC coupled to UV−visible absorption has also been used to detect analytes postseparation. However, despite its high level of sensitivity, UV−visible absorption suffers from the lack of molecular specificity for an analyte.[39] Therefore, in this study we have developed a method to detect MTX and its metabolites in patient urine samples using online LC-SERS, thus taking advantage of SERS as a molecular fingerprinting technique.[40]

MATERIALS AND METHODS

Reagents and Materials. MTX, 7-OH MTX, and DAMPA were purchased from Toronto Research Chemicals (Ontario, Canada). Trisodium citrate, silver nitrate (99.9% purity), potassium nitrate, HPLC grade methanol (MeOH), water, and trifluoroacetic acid (TFA) were purchased from Sigma-Aldrich (Dorset, United Kingdom). Amicon Ultra 0.5 mL centrifugal filters (3 kDa) were purchased from Merck Millipore, Ltd. (Darmstadt, Germany).

Nanoparticles Synthesis. Citrate-reduced silver colloid was synthesis following the Lee and Meisel method.[41] Briefly, silver nitrate (0.09 g) was dissolved in 500 mL of deionized water and heated to boiling. A volume of 10 mL of 1% trisodium citrate in water was added dropwise to a stirring silver nitrate solution, the mixture was left at boiling temperature for ∼30 min. The observation of green-gray colloid is an indication of successful nanoparticle formation. The nanoparticle suspensions were stored covered at room temperature and were useable for several weeks. UV−vis spectrophotometry was used to characterize nanoparticle size distribution to allow comparison of several batches and were similar to data collected earlier and published in refs 42 and 43.

Sample Preparation. Stock solutions (0.5 mM) of MTX, 7-OH MTX, and DAMPA were prepared in 20% methanol. Samples for individual analysis were then prepared by diluting the stock solutions to the appropriate concentration ranging from 0 to 100 μM. Solutions for mixture analysis were prepared in the same way, equal aliquots of each of the relevant analytes were then mixed together (three per mixture), giving the desired final concentrations.

Human Urine Samples. Urine samples were obtained from a healthy volunteer. As detailed in ref 44 midstream first morning samples were collected over several weeks in 50 mL Falcon tubes. Samples were briefly kept at ∼4 °C immediately following collection, then transported to the laboratory, and stored at −80 °C within 2 h of collection. Prior to analysis, 50 mL aliquots were allowed to thaw and centrifuged at 5000g for 10 min at 4 °C, and the supernatant was collected.

In addition, human urine samples were also donated by the Arthritis Research UK Centre for Genetics and Genomics, The University of Manchester. The samples were obtained from patients with Rheumatoid Arthritis (RA) participating in a research study as described previously.[45] The study was approved by a Research Ethics Committee (REC 13/NW/0653) and all contributing patients provided informed consent.

The patients (n = 4) were administered different dosages of MTX (see Table 1). Urine samples were collected over a 24 h period and on two subsequent days within 7 days of MTX administration. Samples were stored at −80 °C until analysis. Prior to analysis, frozen urine was thawed at room temperature and vortex mixed. As previously reported by us for SERS analysis[44,46] to remove protein residues from the urine samples, 300 μL aliquots were transferred onto Amicon Ultra centrifugal filters and centrifuged at 14000g for 30 min following the manufacturer's recommended protocol. 250 μL of filtered urine was then transferred to an Eppendorf tube and concentrated for ∼4 h using vacuum concentration (Eppendorf Vacufuge concentrator 5301, Eppendorf, UK). Once all liquid was evaporated, the sample was resuspended in 125 μL water and vortexed for 8 s, thus increasing the concentration of MTX 2-fold.

Instrumentation. HPLC separation was carried out using a Waters Acquity HPLC system (Waters, Hertfordshire, UK) equipped with a diode array detector. HPLC separation was performed using a Hypersil GOLD (Thermo Scientific, UK) HPLC column with a particle size 1.9 μm, 100 mm length, and 2.1 mm diameter. The mobile phase consisted of water with 0.05% TFA as the aqueous solution (A) and MeOH with 0.05% TFA as the organic component (B). The system was maintained at a flow rate of 0.150 mL min^{-1}. The gradient elution parameters are provided in Table S1.

SERS analysis was achieved using a DeltaNu Advantage portable Raman spectrometer (DeltaNu, Laramie, WY, USA), equipped with a 785 nm HeNe laser. The colloid and aggregation agent for SERS analysis were introduced from a syringe using a syringe pump driver (KD Scientific, Holliston, MA). A syringe of 60 mL silver nanoparticle was introduced to the mobile phase, after mixing 0.5 M of KNO_3 as an aggregation agent was introduced to the mixture from a second syringe driver. Following the introduction of the colloid and aggregation agent, the connection tube of HPLC was positioned in front of the aperture of the Raman spectrometer, where the mixture of mobile phase, colloid and aggregation agent dripped from the tube as the Raman spectrometer recorded and collected spectra of the formation droplet in multiacquire mode. The spectrometry aperture relative to the tube end was optimized via collecting 1 s spectra in continuous mode until the SERS signal response was maximized. A similar protocol of using a liquid droplet including setup of HPLC-

DOI: 10.1021/acs.analchem.7b00916
Anal. Chem. 2017, 89, 6702−6709

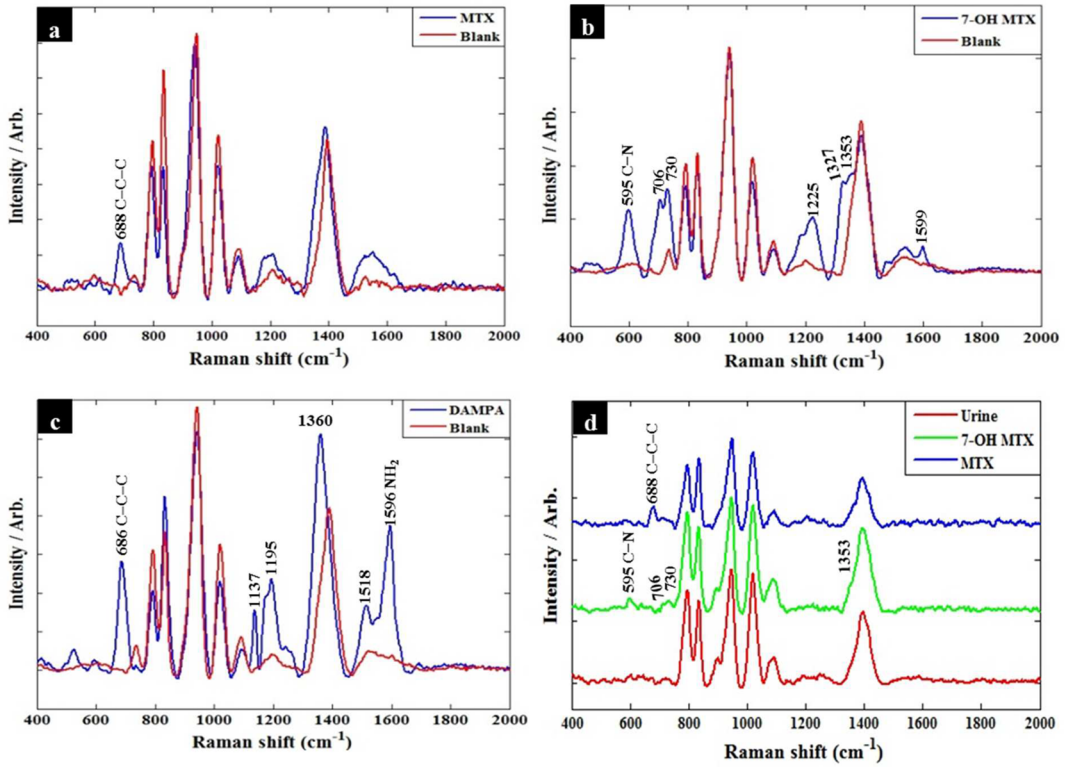

Figure 2. Baseline-corrected SERS spectra (400–2000 cm^{-1}) of (a) MTX, (b) 7-OH MTX, (c) DAMPA (all from standards analyzed by LC individually), and (d) MTX and 7-OH MTX isolated from patients urine samples at their peak retention times (Table 2). In all plots the analyte is shown in blue and green (for panel d only). The mobile phase blank (a–c) or sample in urine (d) is shown in red and these were collected from the same slice of the LC (i.e., at the same RT as the analyte).

SERS has previously been described by.[8] Images of the LC-SERS set up are provided in Figure S1.

LC-SERS Sample Analysis. A volume of 25 μL of each sample was injected onto the LC column and UV absorbance detection was measured at 307 nm. The silver colloid for SERS analysis was pumped at 0.4 mL min^{-1} by a syringe driver, and then mixed with the sample post separation. This mixture was followed by addition of the aggregation agent at the flow rate of 0.1 mL min^{-1}, pumped by a second syringe driver. The colloid and aggregation agent was manually added to the syringes between the end of each sample analysis and the injection of the next, this step did not influence the SERS data (data not shown). After this the eluent-colloid-aggregating agent mixture was analyzed by SERS using multiacquire mode, with an integration time of 1 s.

Data Analysis. All spectral data were analyzed and processed using MATLAB software R2013a (The Math Works Inc., Natwick, U.S.A). The MTX, 7-OH MTX, and DAMPA peak areas at 688, 595, and 1596 cm^{-1} respectively were baseline corrected using asymmetric least-squares (AsLS).[47] These peak areas at different concentration levels were then used to generate three log–log regression models, ($\log_{10}(y) = m\cdot\log_{10}(x) + b$, where y, x, m, and b are the peak area, concentration level, slope of the line and y-intercept, respectively), one for each analyte. No preprocessing was conducted on UV absorbance data and similarly log–log regression models were generated using the log-transformed measured peak areas and the log-transformed concentration levels of the analyte. The reason log–log regression was employed instead of direct linear regression is that the log-transformation had improved the linearity over the whole concentration range.

RESULTS AND DISCUSSION

Initial scoping for the best colloid and aggregating agent (data not shown) established that the optimal conditions for the SERS enhancement of MTX and its metabolites were achieved using citrate-reduced silver colloid with potassium nitrate as the aggregation agent. Prior to application, further optimization of LC-SERS parameters were undertaken to achieve the optimum mixing volumes of the sample, flow rate, Ag colloid, and KNO_3 (data not shown). External syringe drivers were used postcolumn to introduce the silver nanoparticles and aggregation agent to the system, as the use of a more sophisticated liquid delivery instrument could carry contamination risk and the deposition of Ag colloid may damage the internal workings of such instruments. SERS detection was set up downstream to the UV absorbance detector (at 307 nm) such that time taken for the detection of an analyte after accounting for the dwell volume, between the UV detector and the (SERS) laser, was ~130 s later. This delay was taken into consideration for comparison of UV and SERS data for each of the investigated samples.

During sample analysis, sequential SERS spectra were recorded with a 1 s integration time, using the instrument's "multiacquire" setting. With the combined flow rate of 0.65 mL min^{-1}, multiple individual droplets pass in front of the Raman aperture during this collection window for each spectrum. While the instrument starts recording the next spectrum as soon as it has finished the previous collection, it takes approximately 7.5 s (including spectral acquisition) to save

DOI: 10.1021/acs.analchem.7b00916
Anal. Chem. 2017, 89, 6702–6709

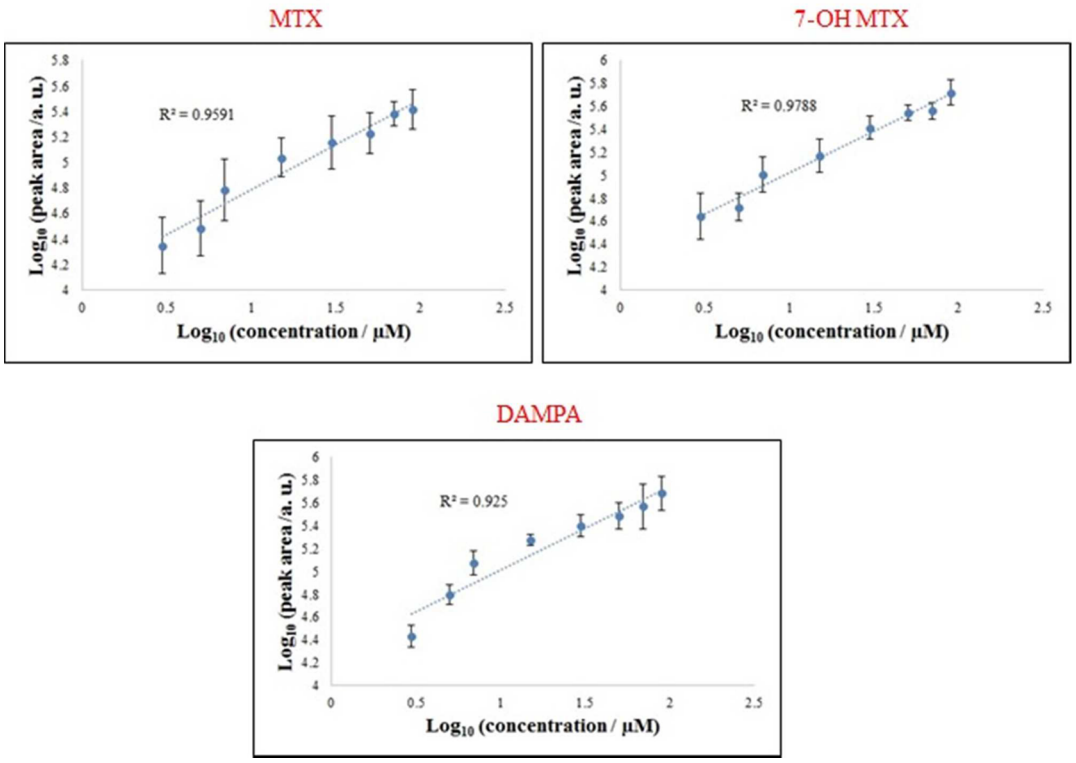

Figure 3. Calibration plots for injections of mixtures of MTX, 7-OH MTX and DAMPA in 20% methanol using SERS detection. The mean SERS peak area (n = 3) is shown with error bars denoting the standard deviation. Insets show a close-up of the main plot in the low concentration region.

the data file, thus a total of 80 scans were recorded over a total acquisition time of 600 s.

The chromatographic conditions were optimized with reversed-phase to separate MTX and its metabolites effectively based on their chemical properties. The chemical structures of these metabolites are shown in Figure 1 and indicate that the detection at 307 nm UV absorbance is achievable.[39] The UV and SERS chromatograms from injections of the individual analytes and the mixture of analytes are shown in (Figure S2) and (Figure S3) respectively. A complete separation of all three analytes can be observed in the UV chromatograms between 4 and 9 min retention time within the total run time of 20 min, which includes a column equilibrium time of 10 min. Organic solvents and gradient elution (Table S1), which are traditionally used for LC separation, are known to interfere with SERS signals and thus this changing background can generate strong Raman scattering which can mask the SERS peaks attributed to the target analytes. However, despite the blank injections varying quantitatively (Figure 2, red spectra) we could generate a clear signal for MTX, with a peak at 688 cm^{-1}, which can be assigned to the C−C−C in aromatic ring.[48] We believe this is the main vibrational band of MTX (Figure 2a), and we have not observed any interference effect from LC solvents when measuring MTX at 688 cm^{-1} in 20% methanol or urine (Figure 2d). A previous study by Hidi et al. using SERS (rather than LC-SERS) demonstrated that MTX binding to the Ag nanoparticles could be via the amino groups within the pteridine ring oriented parallel to the metallic surface,[49] which provides further explanation as to why we detect MTX without any interference from the mobile phase. Figure 2b illustrates the LC-SERS spectra obtained from 7-OH MTX, where the most intense peak at 595 cm^{-1} can be assigned to the C−N vibration. Figure 2c shows the most prominent LC-SERS peaks observed from DAMPA, including peaks at 686, 1137, 1195, 1360, 1518, and 1596 cm^{-1}, which can be assigned to C−C−C in the pteridine ring, C−N, C−H in the aromatic ring, pteridine ring, C−C and NH_2, respectively. Thus, from the LC-SERS spectra (Figure 2) recorded for each of the MTX metabolites, it is evident that SERS signals achieved post separation on the LC column, can be assigned to their corresponding chemical structures (Figure 1), without any background interference from the methanol, water or TFA found in the mobile phase.

Initially we analyzed the three analytes dissolved in 20% methanol individually by LC. Calibration curves from specific vibrational bands for each of the analytes (n = 3 individual injections) were constructed using the total peak areas against concentrations of individual MTX, 7-OH MTX, and DAMPA samples at varying concentrations. These plots were used to calculate the limit of detection (LOD) of each analyte as well as the reproducibility of the UV absorbance and SERS signal (Figures S4 and S5, respectively). When using SERS as the detection method, we observed higher error in the measurement of concentrations above 20 μM. This can be potentially attributed to the saturation of analyte molecules on the nanoparticle surface making repeat measurements or quantitation difficult.[50] However, at concentrations below 20 μM the error is reduced, presumably because of the change in the binding geometry (Figures 3 and S5), thus generating more reliable quantification data.

The LODs for MTX, 7-OH MTX and DAMPA were calculated based on the corresponding regression model[51] in form of $\log_{10}(\text{LOD}) = 3 \times S_{y/x} \div b$ in which $S_{y/x}$ and b are the standard error and slope of the model, respectively. The LODs calculated for MTX, 7-OH MTX and DAMPA were 1.29, 1.84, and 1.31 μM by UV detection and 2.47, 2.87, and 1.66 μM by SERS detection, respectively. Table 2 includes a summary of

DOI: 10.1021/acs.analchem.7b00916
Anal. Chem. 2017, 89, 6702−6709

Table 2. Metrics for HPLC Analysis of Individual and Mixture Samples of MTX and Its Metabolites Dissolved in 20% Methanol Using UV Detection at 307 nm Followed by SERS

detector	analyte	MTX	7-OH MTX	DAMPA
UV	retention time/min	5.34	7.54	8.34
	linearity (R^2) from individual analytes	0.9965	0.9805	0.9961
	linearity (R^2) from analyte mixture	0.9694	0.9864	0.9589
	LOD/μM from individual analytes	1.29	1.84	1.31
	LOD/μM from analyte mixture	2.09	1.63	2.36
SERS	retention time/min	7.44	9.64	10.44
	peak position/cm^{-1}	688	595	1596
	peak assignment	C−C−C aromatic ring	C−N	NH_2
	linearity (R^2) from individual analytes	0.9577	0.9436	0.9865
	linearity (R^2) from analyte mixture	0.9591	0.9788	0.9250
	LOD/μM from individual analytes	2.47	2.87	1.66
	LOD/μM from analyte mixture	2.36	1.84	3.26
LC-UV vs LC-SERS comparisons	linearity (R^2) of predictions from LC-UV vs LC-SERS from individual analytes	0.9787	0.9503	0.9787
	linearity (R^2) of predictions from LC-UV vs LC-SERS from analyte mixture	0.9141	0.9508	0.9068

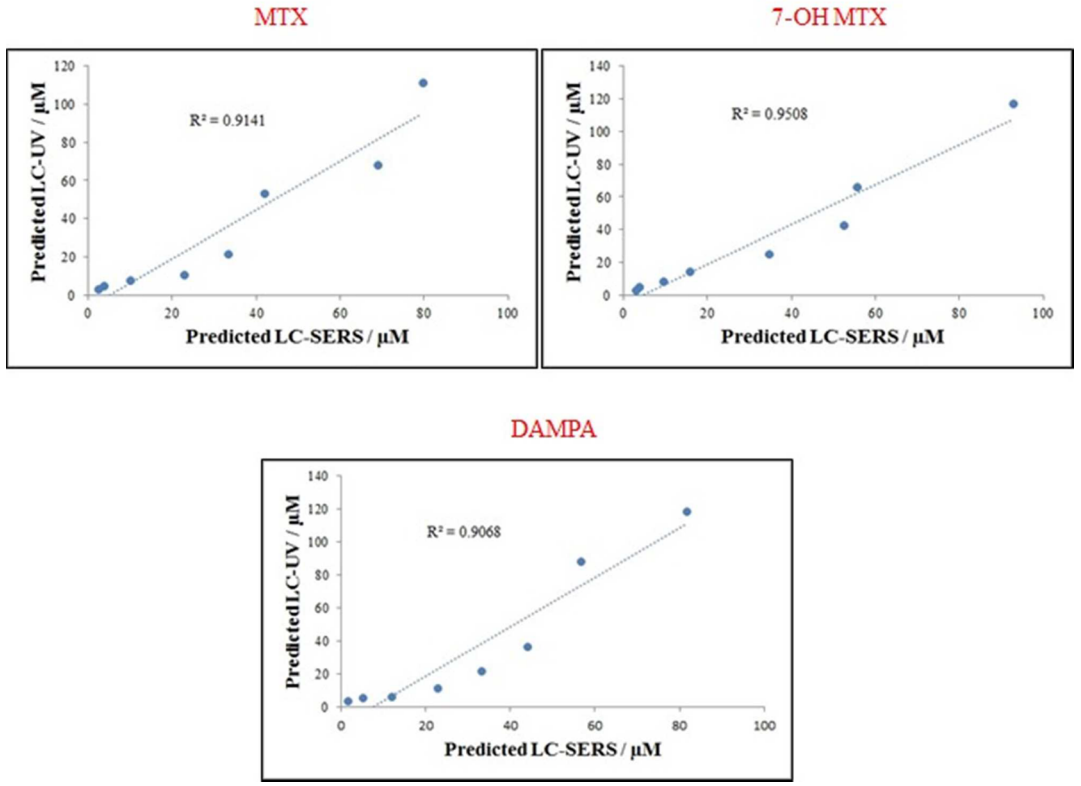

Figure 4. Calibration Plots of predicted LC-UV versus LC-SERS from injections of mixtures of MTX, 7-OH MTX, and DAMPA in 20% methanol. Within each plot the high R^2 indicate that these results are in very good agreement.

the above findings and the relevant vibrational band assignments. Additionally, the plots of UV vs SERS predictions (from individual analyte-specific SERS peaks) are in excellent agreement with each other (Figure S6) and show a strong linear correlation with confirmation reflected in a high R^2 (coefficient of determination, the proportion of the variance in the dependent variable y that is predictable from the independent variable x) values of 0.9787, 0.9503, and 0.9787 calculated for MTX, 7-OH MTX, and DAMPA, respectively (Figure S6).

To examine the ability of this LC-SERS based approach to separate and resolve MTX and its metabolites, mixtures of the three analytes in 20% methanol were also investigated using the same analysis conditions and the same data processing steps. The different retention times and SERS band positions were again observed and used to quantify each of analytes. Note that although we have very good peak separation (Figure S2) the use of SERS compared to UV absorbance data would help resolve closely or coeluting species. Once again, calibration plots for MTX, 7-OH MTX, and DAMPA were generated for both the UV (data not shown) and SERS data (Figure 3), for comparison purposes. As these were mixtures, the definite identification of each analyte by UV was possible due to differences in retention times (Figure S2), followed by analyte-

DOI: 10.1021/acs.analchem.7b00916
Anal. Chem. 2017, 89, 6702−6709

specific spectral profile on SERS (Figure 2), allowing for accurate quantification of individual analytes within a mixture using LC-SERS. The plots of UV vs SERS concentration predictions are presented in Figure 4, and the LOD and calibration linearity data for this mixture analysis are presented in Table 2. It is also noted that the LOD for all the drug and its two metabolites in the mixtures is slightly higher than that recorded for individual analytes for both UV and SERS detections.

Having established for the first time that online LC-SERS can be used to quantify a drug and its metabolites within mixtures (in 20% methanol) successfully, the next stage of analysis looked toward detecting a quantifying MTX, 7-OH MTX, and DAMPA in a complex biological matrix. To achieve this we first spiked urine obtained from a healthy volunteer not exposed to MTX with the three analytes, before finally using calibrations from these models to assess the levels of MTX, 7-OH MTX, and DAMPA in the urine collected from patients undergoing MTX therapy for rheumatoid arthritis.

Thus, MTX and 7-OH MTX were spiked into healthy urine samples to establish calibration curves from these analytes within human urine; DAMPA was not included, as the patients involved in this study had not received the CPDG2 enzyme as a MTX rescue agent (Figure 1). Calibration curves of peak area (of characteristic peaks; namely, 688 and 595 cm^{-1}) against the concentration of the spiked standard were constructed (data not shown). Table S2 summarized the results of the assessment of MTX and 7-OH MTX spiked into urine. The concentrations of MTX and 7-OH MTX in patient's urine samples were then predicted using the linear regression calibrations. The UV chromatograms of MTX spiked into urine, patient urine and healthy urine are shown in Figure S7, which shows that MTX and 7-OH MTX are clearly present in the patient urine. Figure 2d shows the LC-SERS spectra of MTX and 7-OH MTX generated from one of the patient urine samples which are similar to the MTX and 7-OH MTX spectra that were prepared in 20% methanol (Figure 2a and 2b, respectively). Finally, Table 1 provides the results of the assessment of the four patients. While MTX was found in all four patients, its metabolite 7-OH MTX, was found in only two of the samples, and this was detected by both UV and SERS detection. It is clear from this table that the estimated levels from LC-SERS and LC-UV are highly comparable, have low standard deviation (SD) and thus demonstrate excellent reproducibility and precision from real-world human samples.

CONCLUSIONS

This study has demonstrated for the first time the application of online SERS combined with HPLC, for providing real-time data for the quantitative detection of the drug methotrexate and its major metabolites. The introduction of Ag colloid to the postcolumn solvent flow, along with the KNO_3 aggregation agent, provided reproducible SERS spectra for artificial mixtures of MTX, 7-OH MTX, and DAMPA in both 20% methanol and when spiked into human urine from a healthy volunteer who was not exposed to MTX. These molecularly specific Raman spectra also allowed for the quantitative detection of MTX and 7-OH MTX in real patient urine samples with good accuracy, and data were comparable between LC-UV and our novel LC-SERS method. The reversed-phase LC employed gradient elution, which to our knowledge has not been used previously on-line-coupled with SERS for separation and detection of MTX and its metabolites.

This study clearly demonstrates that LC-SERS is a highly promising technique for the detection of MTX in biological fluids. With further optimization to overcome baseline interference from biological compounds, this technique has a potential to screen rapidly for levels within the expected therapeutic range of MTX therapy especially for high-dose MTX cancer treatment. LC-SERS could therefore be used to monitor patient adherence to proposed therapy routines where there may be compliance issues in long-term therapy. Finally, we believe that this approach could be used in combination with MS detection to add additional chemical information on unknown metabolites/analytes, as they are separated from complex samples such as human biofluids and this metabolomics application will be an area for future study.

ASSOCIATED CONTENT

Supporting Information

The Supporting Information is available free of charge on the ACS Publications website at DOI: 10.1021/acs.analchem.7b00916.

Annotated photos of the LC-SERS setup, reversed-phase HPLC conditions used, LC-UV and LC-SERS chromatograms, individual analysis of MTX, 7-OH MTX, and DAMPA that show calibration curves for LC-UV and LC-SERS and a direct comparison of the two methods, LC chromatograms establishing that the method developed works on real patient samples (PDF)

AUTHOR INFORMATION

Corresponding Author

*E-mail: roy.goodacre@manchester.ac.uk.

ORCID

Royston Goodacre: 0000-0003-2230-645X

Notes

(1) Human urine was collected from a single anonymous adult, and no information was collected on this individual. Therefore, for this sample, full ethics following the 1964 Declaration of Helsinki was not required for this study. (2) Urine samples obtained from patients with Rheumatoid Arthritis (RA) did follow the Helsinki Declaration and the study was approved by a Research Ethics Committee (REC 13/NW/0653), and all contributing patients provided informed consent. These samples were provided anonymously to the authors.

The authors declare no competing financial interest.

ACKNOWLEDGMENTS

A.S. thanks the Saudi ministry of high education and Umm al-Qura University for funding. R.G. is indebted to UK BBSRC (BB/L014823/1) for funding for Raman spectroscopy.

REFERENCES

(1) Jorgenson, J. W.; Lukacs, K. D. *Science* **1983**, *222*, 266−272.

(2) Ohno, K. i.; Tachikawa, K.; Manz, A. *Electrophoresis* **2008**, *29*, 4443−4453.

(3) Kaltashov, I. A.; Eyles, S. J. *Mass Spectrom. Rev.* **2002**, *21*, 37−71.

(4) Martin, J. W.; Kannan, K.; Berger, U.; Voogt, P. D.; Field, J.; Franklin, J.; Giesy, J. P.; Harner, T.; Muir, D. C.; Scott, B.; et al. *Environ. Sci. Technol.* **2004**, *38*, 248A−255A.

(5) Strege, M. A. *J. Chromatogr., Biomed. Appl.* **1999**, *725*, 67−78.

(6) Fox, E. J.; Twigger, S.; Allen, K. R. *Ann. Clin. Biochem.* **2009**, *46*, 50−57.

(7) Jessome, L. L.; Volmer, D. A. *LCGC North Am.* **2006**, *24*, 498.

DOI: 10.1021/acs.analchem.7b00916
Anal. Chem. 2017, 89, 6702−6709

(8) Cowcher, D. P.; Jarvis, R.; Goodacre, R. *Anal. Chem.* **2014**, *86*, 9977−9984.
(9) Negri, P.; Schultz, Z. D. *Analyst* **2014**, *139*, 5989−5998.
(10) Kuligowski, J.; Quintás, G.; Garrigues, S.; Lendl, B.; de la Guardia, M. *TrAC, Trends Anal. Chem.* **2010**, *29*, 544−552.
(11) Stiles, P. L.; Dieringer, J. A.; Shah, N. C.; Van Duyne, R. P. *Annu. Rev. Anal. Chem.* **2008**, *1*, 601−626.
(12) Moskovits, M. *Rev. Mod. Phys.* **1985**, *57*, 783.
(13) Ellis, D. I.; Cowcher, D. P.; Ashton, L.; O'Hagan, S.; Goodacre, R. *Analyst* **2013**, *138*, 3871−3884.
(14) Ellis, D. I.; Muhamadali, H.; Haughey, S. A.; Elliott, C. T.; Goodacre, R. *Anal. Methods* **2015**, *7*, 9401−9414.
(15) Campion, A.; Kambhampati, P. *Chem. Soc. Rev.* **1998**, *27*, 241−250.
(16) Dijkstra, R.; Ariese, F.; Gooijer, C.; Brinkman, U. T. *TrAC, Trends Anal. Chem.* **2005**, *24*, 304−323.
(17) Sheng, R.; Ni, F.; Cotton, T. M. *Anal. Chem.* **1991**, *63*, 437−442.
(18) Freeman, R.; Hammaker, R.; Meloan, C.; Fateley, W. *Appl. Spectrosc.* **1988**, *42*, 456−460.
(19) Cabalin, L.; Ruperez, A.; Laserna, J. *Talanta* **1993**, *40*, 1741−1747.
(20) Sägmüller, B.; Schwarze, B.; Brehm, G.; Trachta, G.; Schneider, S. *J. Mol. Struct.* **2003**, *661-662*, 279−290.
(21) Nguyen, A.; Schultz, Z. D. *Analyst* **2016**, *141*, 3630−3635.
(22) Barnhart, K.; Coutifaris, C.; Esposito, M. *Expert Opin. Pharmacother.* **2001**, *2*, 409−417.
(23) Fernández, E. L.; Parés, L.; Ajuria, I.; Bandres, F.; Castanyer, B.; Campos, F.; Farré, C.; Pou, L.; Queraltó, J. M.; To-Figueras, J. *Clin. Chem. Lab. Med.* **2010**, *48*, 437−446.
(24) Graf, N.; Winkler, K.; Betlemovic, M.; Fuchs, N.; Bode, U. *J. Clin. Oncol.* **1994**, *12*, 1443−1451.
(25) Asselin, B. L.; Devidas, M.; Wang, C.; Pullen, J.; Borowitz, M. J.; Hutchison, R.; Lipshultz, S. E.; Camitta, B. M. *Blood* **2011**, *118*, 874−883.
(26) Cronstein, B. N. *Pharmacol. Rev.* **2005**, *57*, 163−172.
(27) Jolivet, J.; Cowan, K. H.; Curt, G. A.; Clendeninn, N. J.; Chabner, B. A. *N. Engl. J. Med.* **1983**, *309*, 1094−1104.
(28) Lennard, L. *Br. J. Clin. Pharmacol.* **1999**, *47*, 131−144.
(29) Crews, K. R.; Liu, T.; Rodriguez-Galindo, C.; Tan, M.; Meyer, W. H.; Panetta, J. C.; Link, M. P.; Daw, N. C. *Cancer* **2004**, *100*, 1724−1733.
(30) Rahiem Ahmed, Y.; Hasan, Y. *J. Cancer Sci. Ther.* **2013**, *5*, 106−112.
(31) Borsi, J. D.; Sagen, E.; Romslo, I.; Moe, P. J. *Med. Pediatr. Oncol.* **1990**, *18*, 217−224.
(32) Klapkova, E.; Kukacka, J.; Kotaska, K.; Suchanska, I.; Urinovska, R.; Prusa, R. *Clin. Lab.* **2011**, *57*, 599.
(33) Donehower, R. C.; Hande, K. R.; Drake, J. C.; Chabner, B. A. *Clin. Pharmacol. Ther.* **1979**, *26*, 63−72.
(34) Widemann, B. C.; Schwartz, S.; Jayaprakash, N.; Christensen, R.; Pui, C. H.; Chauhan, N.; Daugherty, C.; King, T. R.; Rush, J. E.; Howard, S. C. *Pharmacotherapy* **2014**, *34*, 427−439.
(35) Borgman, M. P.; Hiemer, M. F.; Molinelli, A. R.; Ritchie, J. C.; Jortani, S. A. *Ther. Drug Monit.* **2012**, *34*, 193−197.
(36) Pesce, M. A.; Bodourian, S. H. *Ther. Drug Monit.* **1986**, *8*, 115−hyhen.
(37) Mendu, D. R.; Chou, P. P.; Soldin, S. J. *Ther. Drug Monit.* **2007**, *29*, 632−637.
(38) Albertioni, F.; Rask, C.; Eksborg, S.; Poulsen, J. H.; Pettersson, B.; Beck, O.; Schroeder, H.; Peterson, C. *Clin. Chem.* **1996**, *42*, 39−44.
(39) Montemurro, M.; De Zan, M. M.; Robles, J. C. *J. Pharm. Anal.* **2016**, *6*, 103−111.
(40) Ellis, D. I.; Dunn, W. B.; Griffin, J. L.; Allwood, J. W.; Goodacre, R. *Pharmacogenomics* **2007**, *8*, 1243−1266.
(41) Lee, P.; Meisel, D. *J. Phys. Chem.* **1982**, *86*, 3391−3395.
(42) Mabbott, S.; Correa, E.; Cowcher, D. P.; Allwood, J. W.; Goodacre, R. *Anal. Chem.* **2013**, *85*, 923−931.
(43) Westley, C.; Xu, Y.; Carnell, A. J.; Turner, N. J.; Goodacre, R. *Anal. Chem.* **2016**, *88*, 5898.
(44) Subaihi, A.; Almanqur, L.; Muhamadali, H.; AlMasoud, N.; Ellis, D. I.; Trivedi, D. K.; Hollywood, K. A.; Xu, Y.; Goodacre, R. *Anal. Chem.* **2016**, *88*, 10884−10892.
(45) Bluett, J.; Riba-Garcia, I.; Hollywood, K.; Verstappen, S.; Barton, A.; Unwin, R. *Analyst* **2015**, *140*, 1981−1987.
(46) Subaihi, A.; Muhamadali, H.; Mutter, S. T.; Blanch, E.; Ellis, D. I.; Goodacre, R. *Analyst* **2017**, *142*, 1099−1105.
(47) Eilers, P. H. *Anal. Chem.* **2004**, *76*, 404−411.
(48) Ayyappan, S.; Sundaraganesan, N.; Aroulmoji, V.; Murano, E.; Sebastian, S. *Spectrochim. Acta, Part A* **2010**, *77*, 264−275.
(49) Hidi, I.; Mühlig, A.; Jahn, M.; Liebold, F.; Cialla, D.; Weber, K.; Popp, J. *Anal. Methods* **2014**, *6*, 3943−3947.
(50) Faulds, K.; Smith, W. E. *Infrared Raman Spectrosc. Forensic Sci.* **2012**, 357−366.
(51) Shabir, G. A. *J. Chromatogr. A* **2003**, *987*, 57−66.
(52) Bouquié, R.; Deslandes, G.; Nieto Bernáldez, B.; Renaud, C.; Dailly, E.; Jolliet, P. *Anal. Methods* **2014**, *6*, 178−186.
(53) Seideman, P.; Beck, O.; Eksborg, S.; Wennberg, M. *British journal of clinical pharmacology* **1993**, *35*, 409−412.

DOI: 10.1021/acs.analchem.7b00916
Anal. Chem. 2017, 89, 6702−6709